

Abstract

We have improved an ozone Differential Absorption Lidar (DIAL) system, originally developed in March 2010. The improved DIAL system consists of a Nd:YAG laser and a 2 m Raman cell filled with 8.1×10^5 Pa of CO_2 gas which generate four Stokes lines (276, 287, 299, and 312 nm) of stimulated Raman scattering, and two receiving telescopes with diameters of 49 and 10 cm. Using this system, 44 ozone profiles were observed in the 1–6 km altitude range over Saga (33.24° N, 130.29° E) in 2012. High ozone concentration layers were observed at around 2 km altitude during April and May. Ozone (column) amounts within the 1–6 km altitude range were almost constant from January to March, and increased from late April to July. From mid-July through August, ozone column amounts decreased greatly because of exchanges of continental and maritime air masses. Then in mid-September they increased again within 1–6 km, and subsequently decreased slowly, becoming almost constant by December.

The Meteorological Research Institute's Chemistry-Climate Model version 2 (MRI-CCM2) successfully predicted most of these ozone variations with the following exceptions: MRI-CCM2 could not predict the high ozone-mixing ratios measured at around 2 km altitude on 5 May and 11 May, possibly in part because emissions were assumed in the model to be constant (climatological data were used). Ozone-mixing ratios predicted by MRI-CCM2 were low in the 2–6 km range on 7 July and high in the 1–4 km range on 19 July compared with those measured by DIAL.

1 Introduction

Ozone is an important air pollution ~~that~~ at high concentrations ~~damages~~ human health and ecosystems including crops (Parrish et al., 2012). Tropospheric ozone has two sources: photochemical production in the troposphere and downward transport from the stratosphere. Tropospheric ozone is produced from nitrogen oxides (NO_x), carbon monoxide (CO), and volatile organic compounds (VOCs) by photochemical reactions.

173

Abstract { provide mean
in "high" (p. 7)
line 9 : column → provide values in DU
l.10 increased (how much?) (%) how much?
l.12 } → (%) how much?
l.13 } how much?

AMTD

7, 171–194, 2014

DIAL measurement of lower tropospheric ozone

Y. Uchino et al.

Title Page

Abstract

Introduction

Conclusions

References

Tables

Figures

◀

▶

◀

▶

Back

Close

Full Screen / Esc

Printer-friendly Version

Interactive Discussion



More specifically
In Asia, emissions of these ozone precursors increased between 1980 and 2003 (Ohara et al., 2007). In China ~~in particular~~, NO_x increased from 1996 through 2004 (Zhang et al., 2007). Summertime ozone concentrations in the 0–3 km altitude range over Beijing increased at the rate of $3\% \text{ yr}^{-1}$ from 2002 to 2010 (Wang et al., 2012).

Ozone is also a greenhouse gas that plays an important role in climate change. The radiative forcing due to tropospheric ozone is the third strongest after carbon dioxide and methane (IPCC, 2007).

provide citations!
In recent years, high concentrations of surface ozone have been observed from April through June in the Kyushu district of western Japan. In 2011, we deployed an ozone Differential Absorption Lidar (ozone DIAL) system, originally developed by the National Institute for Environmental Studies (NIES) at Tsukuba, at Saga (33.24°N , 130.29°E) in the Kyushu district, with three aims: (1) to validate GOSAT (Greenhouse gases Observing SATellite) ozone products retrieved from thermal infrared spectral radiances by the Thermal And Near infrared Sensor for carbon Observation-Fourier Transform Spectrometer (TANSO-FTS) onboard GOSAT (Ohyama et al., 2012); (2) to detect high ozone concentrations in the lower troposphere; and (3) to compare the observed concentrations with concentration data predicted by the Meteorological Research Institute's (MRI) Chemistry-Climate Model, version 2 (MRI-CCM2) (Deushi and Shibata, 2011). Except in summer, Saga is downwind of the Asian continent most of the year. Thus, if DIAL can be used to detect high ozone concentrations, then inputting DIAL data into MRI-CCM2 will allow us to make useful predictions for photochemical oxidant advisories. In Sect. 2 we describe the ozone DIAL system, including some improvements made since 2011 and comparisons with ozonesonde data, and we describe MRI-CCM2 in Sect. 3. In Sect. 4, we present observational results obtained by the ozone DIAL system and compare them with MRI-CCM2 predictions. Section 5 is a summary and conclusion.

place in page 173 (line 23) after (Parish et al., 2012)

DIAL measurement of
lower tropospheric
ozone

O. Uchino et al.

Title Page

Abstract

Introduction

Conclusions

References

Tables

Figures

◀

▶

◀

▶

Back

Close

Full Screen / Esc

Printer-friendly Version

Interactive Discussion



2 Ozone DIAL system, data analysis and comparison with ozonesonde results

Tropospheric ozone DIAL systems have been developed that use tunable dye lasers (Gibson and Thomas, 1975; Pelon and Megie, 1982; Browell et al., 1983; Proffitt and Langford, 1997; Kuang et al., 2013), ~~and~~ Stokes lines of stimulated Raman scattering (SRS) of pressurized gas pumped by excimer lasers (Uchino et al., 1983; Kempfer et al., 1994; Eisele et al., 1999), and by Nd:YAG lasers (Ancellet et al., 1989; Sunesson et al., 1994; McDermid et al., 2002; Nakazato et al., 2007; Apituley et al., 2010). In 2010, we developed a tropospheric ozone DIAL system at NIES (Uchino et al., 2011) that was installed in a container with dimensions of about 228 cm × 683 cm × 255 cm. The system's transmitter transmits three Stokes lines (276.2 nm, 287.2 nm, and 299.1 nm) of the SRS of carbon dioxide (CO₂) pumped by the fourth harmonic (266 nm) of a Nd:YAG laser (Nakazato et al., 2007; Seabrook et al., 2011).

We used this transmitter with a coaxial receiving system with a 49 cm-diameter Newtonian reflecting telescope to measure ozone profiles from a few hundred meters to about 10 km altitude. However, the signal-induced bias (SIB) from the photomultiplier tubes (PMTs) limited the measurement altitude to below about 6 km (Sunesson et al., 1994; Proffitt and Langford, 1997). A mechanical chopper with a fast rising time could suppress the SIB (Uchino and Tabata, 1991; McDermid et al., 2002; Godin-Beekmann et al., 2003; Apituley et al., 2010), but there is not enough space in the container to add a mechanical chopper to the DIAL receiving system. Therefore, in January 2012 we modified the coaxial receiving system by adding a biaxial system. In the biaxial system, the Stokes lines were transmitted upward by a 10 cm-diameter mirror with 90% reflectivity that was set at a distance of 25 cm from the edge of the 49 cm telescope, and about 10% of the laser energy was used to measure low-altitude ozone by the original coaxial system. By adding the biaxial system, we could measure ozone profiles up to about 10 km; but it was time-consuming to measure ozone profiles from 1 to 10 km by alternating between biaxial and coaxial measurements.

AMTD

7, 171–194, 2014

DIAL measurement of lower tropospheric ozone

O. Uchino et al.

Title Page

Abstract

Introduction

Conclusions

References

Tables

Figures

◀

▶

◀

▶

Back

Close

Full Screen / Esc

Printer-friendly Version

Interactive Discussion



* Later,

175

add:

"e.g.

Papayannis et al., 1990)

Tzortzakis et al., 2004 (Appl. Phys. B 79, 71–76)

with vibrational shift of cm⁻¹

Augeo
Papayannis et al., 2005
Annales Geophys.

23, 2039–2050

[Table 1]

an additional

be able

To make it possible to measure tropospheric ozone profiles simultaneously in the altitude range of 0.3–10 km, we introduced a new 10 cm-diameter Newtonian reflecting telescope in September 2012, using a 1.8 mm-diameter quartz optical fiber cable to transmit the receiving light from the position of the iris of the 10 cm telescope to the entrance of a spectrometer. A dichroic beamsplitter with a 15° incidence angle efficiently separated the signal into two wavelengths, 276 and 287 nm. Furthermore, we tested the use of a fourth Stokes line (312.0 nm) of SRS from CO₂ for measurement of ozone up to 15–20 km on a clear night.

A block diagram of the improved DIAL system is shown in Fig. 1. The maximum output pulse energy of the Nd:YAG laser (Quintel YG981C) is 107 mJ per pulse at 266 nm; however, the normal averages of the output energies are 70–85 mJ. The laser beam is collimated into the center of a 2 m-long Raman cell, which consists of a stainless-steel tube with a diameter of 35 mm and 10 mm-thick UV-grade quartz windows with an anti-reflective (AR) coating. The input window is a lens with a focal length $f_1 = 1100$ mm. The output energy at 312.0 nm is not measured, but CO₂ pressure is set to be 8.1×10^5 Pa because the largest receiving signal is obtained at 312.0 nm. At 8.1×10^5 Pa of CO₂ pressure, the output energies of the three Stokes lines at 276.2, 287.2, and 299.1 nm are 7.5, 9.1, and 8.4 mJ, respectively. A pumping energy of more than 90 mJ at 266 nm is necessary for DIAL measurement using the Stokes lines at 299 nm and 312 nm.

The four Stokes lines are expanded by a factor of about 3.9 by a 50 mm-diameter quartz lens with a focal length $f_2 = 4290$ mm. The beam divergence of the four Stokes lines transmitted into the atmosphere is about 0.1 mrad. The full field of views of the 49 cm and 10 cm telescope are 1.0 and 3.0 mrad, respectively. The system uses PMTs (Hamamatsu R3235) to detect the backscattered light from the atmosphere. For signal processing, a 12-bit A/D converter and photon counter (Licel TR20-160) are used. The timing of the DIAL system is controlled by a delay pulse generator (Stanford Research Systems DG645). The specifications of this ozone DIAL system are summarized in Table 1.

AMTD

7, 171–194, 2014

DIAL measurement of lower tropospheric ozone

O. Uchino et al.

Title Page	
Abstract	Introduction
Conclusions	References
Tables	Figures
◀	▶
◀	▶
Back	Close
Full Screen / Esc	
Printer-friendly Version	
Interactive Discussion	



176

Due to the weak available energy at the 4th Stokes line (S_4) at 312 nm, we should use pump energies exceeding 90 mJ.

at 266 nm, which is then used to pump

70–85 mJ

Energy stability for 6 hrs?

problem:

I am afraid 1 single lens is not enough for such a wide spectral range (chromatic aberration)

provide comment please

276 → 312 nm

The ozone number density is derived from the DIAL signals at ~~two~~ ^{two} wavelengths. The raw data were obtained with ~~7.5 m range bin~~ ^{7.5 m range bin} and ~~21 min~~ ^{21 min} integration time (i.e., 600 shots). The analog and photon counting signals for each receiving wavelength channel in Fig. 1 were connected to gain high dynamic range. To increase the signal-to-noise ratio, the integrated spatial range interval (Δz) was varied from 75 to 375 m with altitude. Ozone number concentration profiles were computed from the differential of the logarithm of the ratio of the signals by fitting a third-order polynomial to nine adjacent signals by the least-mean-squares method (Fujimoto and Uchino, 1994). The effective vertical resolution was about $9 \cdot \Delta z \cdot 0.4 = 3.6 \cdot \Delta z$, which was estimated from the full-width half-maximum of the ozone profiles retrieved when an impulse function of ozone density was input (Beyerle and McDermid, 1999). To calculate atmospheric molecular extinction, we used the atmospheric molecular extinction cross section (Bucholtz, 1995) and the atmospheric molecular density obtained from radiosonde data at the Fukuoka District Meteorological Observatory (33.58° N, 130.38° E). The ozone absorption cross section ~~was~~ ^{is} calculated by taking temperature dependence into account (Bass, 1984). The ozone mixing ratio was also calculated from the molecular density, including water vapor.

An example of DIAL measurements using four wavelengths, including 312 nm, is shown in Fig. 2. In this case, vertical profiles of the ozone number density and mixing ratio are plotted with their statistical errors (precision) calculated from the lidar signal-to-noise ratios (Uchino and Tabata, 1991). A different wavelength pair was used for each of three altitude ranges: 276/288 nm for 0.0–3.0 km ($\Delta z = 75$ m), 287/299 nm for 1.6–8.0 km ($\Delta z = 150$ m) and 8.0–18.6 km ($\Delta z = 375$ m), and 299/312 nm for 17.4–20.8 km ($\Delta z = 375$ m). The integration time was about 6 h to observe vertical profiles of the ozone number density and mixing ratio up to 20 km as shown in Fig. 2, but vertical profiles of them up to 6 km were obtained within 30 min. From January through September 2012, we generally used an integration time of about 1–3 h ~~each~~ ^{each} for biaxial and coaxial DIAL measurements, and the resulting measurement errors were larger than those shown in Fig. 2. In this paper, we present the 2012 ozone data for below

[Weikamp, 2005]
AMTD
7, 171–194, 2014

DIAL measurement of lower tropospheric ozone

O. Uchino et al.

Title Page	
Abstract	Introduction
Conclusions	References
Tables	Figures
◀ ▶	
◀ ▶	
Back	Close
Full Screen / Esc	
Printer-friendly Version	
Interactive Discussion	



0.3

177

set to

altitudes lower than

To adapt to different ozone optical depths

Browell et al (1983),
Papayannis et al. 1990
Appl. Opt. 29, 467–476, 1990

Appl. Opt. 22(4), 522–534
update... more recent ones

and to 30 min from 0.3 to 6 km.

6 km, measured by the DIAL system using three wavelengths (276, 287, and 299 nm). In this DIAL data analysis, the systematic error (accuracy) due to particulate backscatter and extinction was not taken into account. The systematic error is ~~probably~~ ^{generally} on the order of 10–15% in the planetary boundary layer and smaller than that in the free troposphere (Nakazato et al., 2007). ^{However} ~~although it can reach very high values~~

We compared DIAL measurement ^{data} and ozonesonde ^{data} (Thompson et al., 2011) (Fig. 3). The ozonesondes used were composed of an ECC ozone sensor (ENSCI-Z) and a GPS radiosonde (Meisei RS-06G). The precision and accuracy of the ozone sensor were $\pm 4\%$ and $\pm 5\%$ at 1000 hPa and $\pm 12\%$ and $\pm 12\%$ at 200 hPa, respectively, and the vertical resolution of the sensor was 300 m (http://www.dropletmeasurement.com/products/airborne/ECC_Ozonesonde). Two ozonesondes were launched by the Japan Weather Association under contract with NIES, and the measurements used in our comparison were made on 9 and 15 January 2013. The ozonesonde and DIAL measurement times were from 12:31 to 13:53 LT and from 12:46 to 13:30 LT, respectively, on 9 January. On 15 January, the ozonesonde measurement time was from 12:31 to 14:04 LT under cloudy conditions, and we used DIAL data obtained from 14:00 to 17:04 LT under comparatively clear weather conditions for the comparison. The vertical ^{range} resolution of the DIAL measurement was 110 m in the lower altitude range and 830 m in the upper altitude range. Within their measurement errors, the ozonesonde and DIAL data were consistent below an altitude of 6 km (Fig. 3).

3 MRI-CCM2

^{The} MRI-CCM2 ^{model} uses chemical and physical processes from the surface to the stratosphere to simulate the global distribution and evolution of ozone and other trace gases (Deushi and Shibata, 2011). The previous version (MRI-CCM1) was a stratospheric chemistry-climate model (Shibata et al., 2005). Version 2, however, incorporates an elaborate mechanism for HO_x - NO_x - CH_4 -CO photochemistry and mechanisms for the

178

(2.9%) in case of AMTD dust aerosol presence
7, 171–194, 2014
(Papayannis et al., 1990)

DIAL measurement of lower tropospheric ozone
O. Uchino et al.

Discussion Paper | Discussion Paper | Discussion Paper | Discussion Paper | Discussion Paper

7101500; 1990

Title Page	
Abstract	Introduction
Conclusions	References
Tables	Figures
◀	▶
◀	▶
Back	Close
Full Screen / Esc	
Printer-friendly Version	
Interactive Discussion	

CC BY

→ Papayannis A, et al, Appl Opt. 29 (4)
467–476 (1990)

degradation of non-methane hydrocarbons and heterogeneous tropospheric reactions of aerosols, so it can simulate tropospheric ozone chemistry as well as stratospheric chemistry. Deushi and Shibata (2011) showed that MRI-CCM2 can reproduce reasonably well the observed seasonal variations of the monthly means of ozone and carbon monoxide in the troposphere. This model is currently used to predict the distribution of photochemical oxidants near the surface in support of operational air-quality forecasts of the Japan Meteorological Agency (JMA). As first step toward better air quality prediction using the model, it is necessary to evaluate MRI-CCM2 by various observational data. It is important to compare ozone data predicted by the model with not only surface ozone data but also vertical ozone data.

The chemistry module of MRI-CCM2 considers 90 chemical species, 231 homogeneous gas-phase chemical reactions (172 chemical kinetic reactions and 59 photolysis reactions), and 16 heterogeneous reactions, and it incorporates grid-scale transport with a semi-Lagrangian scheme, sub-grid-scale convective transport and turbulent diffusion, dry and wet deposition, and emissions of trace gases from various sources. The chemistry module is coupled with an MRI atmospheric general circulation model (MRI-AGCM3; Yukimoto et al., 2011) via a simple coupler (Yoshimura and Yukimoto, 2008). The chemistry module receives meteorological and radiation fields and surface conditions from MRI-AGCM3. The horizontal coordinate system of MRI-CCM2 is a Gaussian grid with a resolution of about 110 km. In the vertical, a hybrid p - σ coordinate system is used, with 48 layers from the surface to the top of the atmosphere (0.01 hPa \approx 80 km). In the hybrid p - σ coordinate system, the vertical coordinate is a terrain-following σ -coordinate ($\sigma = p/p_s$) near the surface, and it gradually changes to a pressure coordinate (p -coordinate) near the top. The vertical resolution increases from about 100 to 600 m from the surface to 6 km. The time step of the transport (chemistry) scheme is 30 (15) min.

In this study, the horizontal wind field in AGCM3 was forced toward the observed field by using a nudging assimilation with an 18 h e-folding time. JMA operational analysis data were used as the observed wind field for the nudging assimilation. In the

DIAL measurement of
lower tropospheric
ozone

O. Uchino et al.

Title Page

Abstract

Introduction

Conclusions

References

Tables

Figures

◀

▶

◀

▶

Back

Close

Full Screen / Esc

Printer-friendly Version

Interactive Discussion



chemistry module, trace gas emissions from the burning of fossil fuels by industrial activities and aircraft (anthropogenic sources), from biomass burning (anthropogenic and natural sources), and from vegetation, soils, and the ocean (natural sources) were prescribed. Global anthropogenic emission data, except those from East Asia, were obtained from the inventory in the Emission Database for Global Atmospheric Research (EDGAR) v2.0 (Olivier et al., 1996) modified by the seasonal adjustments of Müller (1992). For East Asia, the prescribed data were obtained from an inventory of Asian anthropogenic emissions, the Regional Emission inventory in ASia (REAS), version 1.1 (Ohara et al., 2007). Biogenic and oceanic emissions were taken from Horowitz et al. (2003) and references therein. Emission of NO_x from lightning was diagnosed at 6 h intervals in the chemistry module by using the meteorological fields from AGCM3 (for details, see Deushi and Shibata, 2011). Emission of trace gases from biomass burning, which depends on the height above ground, is based on the Description of EDGAR 32FT2000(v8) ([http://www.rivm.nl/edgar/Images/Description_of_EDGAR_32FT2000\(v8\)_tcm32-22222.pdf](http://www.rivm.nl/edgar/Images/Description_of_EDGAR_32FT2000(v8)_tcm32-22222.pdf)). Present-day concentrations of N_2O , CH_4 , chlorofluorocarbons, and halons were prescribed at the surface. We used the data output by the model every hour for the comparison with the DIAL-observed data in this study.

4 DIAL observational results and comparison with MRI-CCM2 output

Hourly grid-point ozone data predicted by MRI-CCM2 were spatially interpolated to Saga, averaged over the DIAL measurement time (about 1–7 h), and then compared with DIAL ozone data.

4.1 Vertical profiles

The vertical profiles of lower tropospheric ozone in an altitude range of 1–6 km measured by DIAL between January and May 2012 are compared with MRI-CCM2 predictions in Fig. 4. The DIAL-measured ozone mixing ratios on 30 January, which were

DIAL measurement of lower tropospheric ozone

O. Uchino et al.

Title Page

Abstract

Introduction

Conclusions

References

Tables

Figures

◀

▶

◀

▶

Back

Close

Full Screen / Esc

Printer-friendly Version

Interactive Discussion



hrs

now observation —

180 volume

being of

the

for the

to our

area

At first

about 40–50 ppb throughout the altitude range, were successfully predicted by MRI-CCM2, except in the 4–5 km altitude range. High ozone-mixing ratios were measured at around 2 km altitude in the daytime on 23 April, 5 May, and 11 May. The results of a backward trajectory analysis suggested that the air masses with these high ozone-mixing ratios at 2 km were transported to Saga across the Yellow Sea (23 April and 5 May) or over the Korean Peninsula (11 May) from polluted areas in East China (Parrish and Zhu, 2009) within a few days. MRI-CCM2 predicted well the high ozone densities on 23 April, but not those on 5 May or 11 May. This is possibly in part because emissions were assumed in the model to be constant (climatological data were used).

Figure 5 shows ozone profiles in the 1–6 km altitude range for July and September 2012. MRI-CCM2 was unable to predict the high ozone-mixing ratios of more than 70 ppb above 2.3 km that were measured by DIAL on 7 July. On 19 July, the measured ozone-mixing ratios were 10–30 ppb below about 4 km, whereas MRI-CCM2 predicted ratios of 30–40 ppb below 4 km. On 28 July, however, MRI-CCM2 predicted well the ozone-mixing ratios measured by DIAL of about 35–70 ppb from 500 m to 6 km. According to the backward trajectory analysis of the air masses, the air masses below 4 km (with low ozone-mixing ratios on 19 and 28 July) came from the Pacific Ocean south of Saga. The ozone-mixing ratios predicted by MRI-CCM2 for 2–6 km on 7 July were lower, and those for 1–4 km on 19 July were higher, compared with the DIAL measurements. A regional model with a higher spatial resolution of 20 km might solve these discrepancies.

4.2 Lower tropospheric ozone column

Figure 6 shows time variations of the lower tropospheric ozone column amounts within the 1–6 km and 1–2 km altitude ranges over Saga in 2012 as measured by DIAL and predicted by MRI-CCM2. Because of weather conditions, DIAL measurements were obtained only twice in May and twice in June, but at least three measurements were obtained in each of the other months. In 2012, the ozone

181

values linked

AMTD

7, 171–194, 2014

DIAL measurement of lower tropospheric ozone

O. Uchino et al.

Volume

Title Page

Abstract Introduction

Conclusions References

Tables Figures

◀ ▶

◀ ▶

Back Close

Full Screen / Esc

Printer-friendly Version

Interactive Discussion

CC BY

restricting

of ~20–40 ppb

According to these comparisons

and better emissions inventory

column amounts showed an approximately seasonal variation except for a dip from early July through mid-September. Column amounts within 1–6 km were almost constant from January to early March, and then increased until late June. The maximum value in the 1–6 km range was 7.82×10^{21} molecules m^{-2} , corresponding to 29.1 DU (1 DU = 2.688×10^{20} molecules m^{-2}), on 22 June 2012. Thereafter, ozone column amounts within the 1–6 km range decreased to early August, but with large variations. The minimum value within the 1–6 km range of 2.28×10^{21} molecules m^{-2} (8.5 DU) was observed on 15 August 2012. These variations are due to exchanges between the ozone-rich continental air mass and the ozone-poor maritime air mass. Subsequently, ozone column amounts increased again to mid-September, and then decreased slowly, becoming almost constant by December, when the ozone column amount within the 1–6 km range was 4.65×10^{21} molecules m^{-2} (17.3 DU). The results predicted by MRI-CCM2 were mainly consistent with these DIAL observational results. The temporal variation of the ozone column amounts within the 1–2 km range in 2012 was similar to that in the 1–6 km range. The mean value was about 1.03×10^{21} molecules m^{-2} (3.8 DU) from 20 January to 11 February. Then, the ozone column amount increased to a maximum value of 2.02×10^{21} molecules m^{-2} (7.5 DU) on 5 May, followed by a decrease to a minimum value of 0.32×10^{21} molecules m^{-2} (1.1 DU) on 19 July. The mean ozone column amount within the 1–2 km range was about 0.55×10^{21} molecules m^{-2} (2.0 DU) from 28 July to 18 August. Subsequently, the value increased to more than 1.0×10^{21} molecules m^{-2} (3.7 DU) by 19 December. MRI-CCM2 predicted similar variations of the ozone column amounts within the 1–2 km range, but the predicted values were lower than the DIAL measurements on 5 and 11 May and 22 June.

AMTD

7, 171–194, 2014

DIAL measurement of lower tropospheric ozone

O. Uchino et al.

Title Page

Abstract

Introduction

Conclusions

References

Tables

Figures

◀

▶

◀

▶

Back

Close

Full Screen / Esc

Printer-friendly Version

Interactive Discussion



Moreover
column ozone
column ozone

5 Concluding remarks

- With ^{our} the improved DIAL system, 44 ozone profiles were observed in the 1–6 km altitude range over Saga in 2012. High ozone-mixing ratios were observed at around 2 km altitude during April and May. Ozone column amounts within the 1–6 km altitude range were almost constant from January to March, and they increased from late April to July. From mid-July through August, ozone column amounts showed large variations, attributed to exchanges between continental and maritime air masses. Ozone column amounts within the 1–6 km range increased again to mid-September, then decreased slowly and became almost constant through December.
- MRI-CCM2 successfully predicted these ozone variations with the following exceptions. MRI-CCM2 could not predict the high ozone-mixing ratios measured at around 2 km altitude on 5 May and 11 May, possibly in part because emissions (especially from open biomass burning) were assumed in the model to be constant (climatological data were used). Ozone-mixing ratios predicted by MRI-CCM2 were low in the 2–6 km range on 7 July and high in the 1–4 km range on 19 July compared with those measured by DIAL. MRI-CCM2 is a global model with a horizontal resolution of about 110 km. Use of a regional model such as MRI-PM/c (Kajino et al., 2012) with a higher spatial resolution of 20 km, an up-to-date inventory, and a higher time resolution of biomass burning emissions should decrease the differences between predicted and measured ozone.
- Acknowledgements. We used radiosonde data measured by the Japan Meteorological Agency, and the Meteorological Data Explorer (METEX), developed by Jiye Zeng at the Center for Global Environmental Research (CGER) of NIES to calculate isentropic backward trajectories. This work was partly supported by JSPS KAKENHI Grant Number 23310018.

183

PS: In your concluding remarks some numerical values (results) are missing
Please add

AMTD

7, 171–194, 2014

DIAL measurement of lower tropospheric ozone

O. Uchino et al.

Title Page

Abstract

Introduction

Conclusions

References

Tables

Figures

◀

▶

◀

▶

Back

Close

Full Screen / Esc

Printer-friendly Version

Interactive Discussion



References

- Ancellet, G., Papayannis, A., Pelon, J., and Megie, G.: DIAL tropospheric ozone measurement using a Nd:YAG laser and the Raman shifting technique, *J. Atmos. Ocean. Tech.*, 6, 832–839, 1989.
- 5 Apituley, A., Hoexum, M., Potma, C., and Wilson, K.: Tropospheric ozone DIAL for air quality and climate monitoring, and validation studies, in: *Proceedings of the 25th International Laser Radar conference*, St.-Petersburg, 5–9 July 2010, 862–865, 2010.
- Bass, A. M.: *The Ultraviolet Absorption Cross-Section of Ozone*, Fin. Rep. NASA, Cont. No. S-40127B, 1984.
- 10 Beyerle, G. and McDermid, I. S.: Altitude range resolution of differential absorption lidar ozone profiles, *Appl. Optics*, 38, 924–927, 1999.
- Browell, E. V., Carter, A. F., Shipley, S. T., Allen, R. J., Butler, C. F., Mayo, M. N., Siviter Jr., J. H., and Hall, W. M.: NASA multipurpose airborne DIAL system and measurements of ozone and aerosol profiles, *Appl. Optics*, 22, 522–534, 1983.
- 15 Bucholtz, A.: Rayleigh-scattering calculations for the terrestrial atmosphere, *Appl. Optics*, 34, 2765–2773, 1995.
- Deushi, M. and Shibata, K.: Development of a meteorological research institute chemistry-climate model version 2 for the study of tropospheric and stratospheric chemistry, *Pap. Meteorol. Geophys.*, 62, 1–46, doi:10.2467/mripapers.62.1, 2011.
- 20 Eisele, H., Scheel, H. E., Sladkovic, R., and Trickl, T.: High-resolution lidar measurements of stratosphere-troposphere exchange, *J. Atmos. Sci.*, 319–330, 1999.
- Fujimoto, T. and Uchino, O.: Estimation of the error caused by smoothing on DIAL measurements of stratospheric ozone, *J. Meteorol. Soc. Jpn.*, 72, 605–611, 1994.
- Gibson, A. J. and Thomas, L.: Ultraviolet laser sounding of the troposphere and lower stratosphere, *Nature*, 256, 561–563, 1975.
- 25 Godin-Beekmann, S., Porteneuve, J., and Garnier, A.: Systematic DIAL lidar monitoring of the stratospheric ozone vertical distribution at Observatoire de Haute-Provence (43.92° N, 5.71° E), *J. Environ. Monitor.*, 5, 57–67, 2003.
- Horowitz, L. W., Walters, S. M., Mauzerall, D. L., Emmons, L. K., Rasch, P. J., Granier, C., Tie, X., Lamarque, J.-F., Schultz, M. G., Tyndall, G. S., Orlando, J. J., and Brasseur, G. P.: A global simulation of tropospheric ozone and related tracers: description and evaluation of MOZART, version 2, *J. Geophys. Res.*, 108, 4784, doi:10.1029/2002JD002853, 2003.
- 30

DIAL measurement of lower tropospheric ozone

O. Uchino et al.

Title Page

Abstract

Introduction

Conclusions

References

Tables

Figures

◀

▶

◀

▶

Back

Close

Full Screen / Esc

Printer-friendly Version

Interactive Discussion



- Intergovernmental Panel on Climate Change (IPCC): Climate change 2007: The Physical Science Basis: Contribution of Working Group I to the Fourth Assessment Report of the Intergovernmental Panel on Climate Change, edited by: Solomon, S., Qin, S., Manning, M., Chen, Z., Marquis, M., Averyt, K. B., Tignor, M., and Miller, H. L., Cambridge University Press, Cambridge, UK and New York, NY, USA, 996 pp., 2007.
- Kajino, M., Deushi, M., Maki, T., Oshima, N., Inomata, Y., Sato, K., Ohizumi, T., and Ueda, H.: Modeling wet deposition and concentration of inorganics over Northeast Asia with MRI-PM/c, *Geosci. Model Dev.*, 5, 1363–1375, doi:10.5194/gmd-5-1363-2012, 2012.
- Kempfer, U., Carnuth, W., Lotz, R., and Trickl, T.: A wide-range ultraviolet lidar system for tropospheric ozone measurements: development and application, *Rev. Sci. Instrum.*, 65, 3145–3164, 1994.
- Kuang, S., Newchurch, M. J., Burris, J., and Liu, X.: Ground-based lidar for atmospheric boundary layer ozone measurements, *Appl. Optics*, 52, 3557–3566, 2013.
- McDermid, I. S., Beyers, G., Haner, D. A., and Leblanc, T.: Redesign and improved performance of the tropospheric ozone lidar at the Jet Propulsion Laboratory Table Mountain Facility, *Appl. Optics*, 41, 7550–7555, 2002.
- Müller, J. F.: Geographical distribution and seasonal variation of surface emissions and deposition velocities of atmospheric trace gases, *J. Geophys. Res.*, 97, 3787–3804, 1992.
- Nakazato, M., Nagai, T., Sakai, T., and Hirose, Y.: Tropospheric ozone differential-absorption lidar using stimulated Raman scattering in carbon dioxide, *Appl. Optics*, 46, 2269–2279, 2007.
- Ohara, T., Akimoto, H., Kurokawa, J., Horii, N., Yamaji, K., Yan, X., and Hayasaka, T.: An Asian emission inventory of anthropogenic emission sources for the period 1980–2020, *Atmos. Chem. Phys.*, 7, 4419–4444, doi:10.5194/acp-7-4419-2007, 2007.
- Ohyama, H., Kawakami, S., Shiomi, K., and Miyagawa, K.: Retrievals of total and tropospheric ozone from GOSAT thermal infrared spectral radiances, *IEEE T. Geosci. Remote Sens.*, 50, 1770–1784, doi:10.1109/TGRS.2011.2170178, 2012.
- Olivier, J. G. J., Bouwman, A. F., van der Maas, C. W. M., Berdowski, J. J. M., Veldt, C., Bloos, J. P. J., Visschedijk, A. J. H., Zandveld, P. Y. J., and Haverlag, J. L.: Description of EDGAR version 2.0: a set of global emission inventories of greenhouse gases and ozone-depleting substances for all anthropogenic and most natural sources on a per country basis and on $1^\circ \times 1^\circ$ grid, RIVM Rep. 771060 002/TNO-MEP Rep. R96/119, National Institute of Public Health and Environment, Bilthoven, Netherlands, 1996.

DIAL measurement of lower tropospheric ozone

O. Uchino et al.

Title Page

Abstract

Introduction

Conclusions

References

Tables

Figures

I◀

▶I

◀

▶

Back

Close

Full Screen / Esc

Printer-friendly Version

Interactive Discussion



- Parrish, D. D. and Zhu, T.: Clean air for megacities, *Science*, 326, 674–675, doi:10.1126/science.1176064, 2009.
- Parrish, D. D., Law, K. S., Staehelin, J., Derwent, R., Cooper, O. R., Tanimoto, H., Volz-Thomas, A., Gilge, S., Scheel, H.-E., Steinbacher, M., and Chan, E.: Long-term changes in lower tropospheric baseline ozone concentrations at northern mid-latitudes, *Atmos. Chem. Phys.*, 12, 11485–11504, doi:10.5194/acp-12-11485-2012, 2012.
- Pelon, J. and Megie, G.: Ozone monitoring in the troposphere and lower stratosphere: evaluation and operation of a ground-based lidar station, *J. Geophys. Res.*, 87, 4947–4955, 1982.
- Proffitt, M. H. and Langford, A. O.: Ground-based differential absorption lidar system for day or night measurements of ozone throughout the free troposphere, *Appl. Optics*, 36, 2568–2585, 1997.
- Seabrook, J. A., Whiteway, J., Staebler, R. M., Bottenheim, J. W., Komguem, L., Gray, L. H., Barber, D., and Asplin, M.: LIDAR measurements of Arctic boundary layer ozone depletion events over the frozen Arctic Ocean, *J. Geophys. Res.*, 116, D00S02, doi:10.1029/2011JD016335, 2011.
- Shibata, K., Deushi, M., Sekiyama, T. T., and Yoshimura, H.: Development of an MRI chemical transport model for the study of stratospheric chemistry, *Pap. Meteorol. Geophys.*, 55, 75–119, 2005.
- Sunesson, J. A., Apituley, A., and Swart, D. P. J.: Differential absorption lidar system for routine monitoring of tropospheric ozone, *Appl. Optics*, 33, 7045–7058, 1994.
- Thompson, A. M., Oltmans, S. J., Tarasick, D. W., Von der Gathen, P., Smit, H. G. J., and Witte, J. C.: Strategic ozone sounding networks: review of design and accomplishments, *Atmos. Environ.*, 45, 2145–2163, 2011.
- Uchino, O. and Tabata, I.: Mobile lidar for simultaneous measurements of ozone, aerosols, and temperature in the stratosphere, *Appl. Optics*, 30, 2005–2012, 1991.
- Uchino, O., Tokunaga, M., Maeda, M., and Miyazoe, Y.: Differential-absorption-lidar measurement of tropospheric ozone with excimer-Raman hybrid laser, *Opt. Lett.*, 8, 347–349, 1983.
- Uchino, O., Sakai, T., Nagai, T., Nakazato, M., Morino, I., Yokota, T., Matsunaga, T., Sugimoto, N., Arai, K., and Okumura, H.: Development of a mobile lidar for GOSAT product validation, *J. Remote Sens. Soc. Jpn.*, 31, 435–445, 2011 (in Japanese).
- Wang, Y., Konopka, P., Liu, Y., Chen, H., Müller, R., Plöger, F., Riese, M., Cai, Z., and Lü, D.: Tropospheric ozone trend over Beijing from 2002–2010: ozonesonde measurements and modeling analysis, *Atmos. Chem. Phys.*, 12, 8389–8399, doi:10.5194/acp-12-8389-2012, 2012.

add:

Stohl, A., et al. (2003) → doi:10.1029/2002JD002490.56

DIAL measurement of lower tropospheric ozone

O. Uchino et al.

Title Page

Abstract

Introduction

Conclusions

References

Tables

Figures

◀

▶

◀

▶

Back

Close

Full Screen / Esc

Printer-friendly Version

Interactive Discussion



- Yoshimura, H. and Yukimoto, S.: Development of a simple coupler (Scup) for Earth system modeling, *Pap. Meteorol. Geophys.*, 59, 19–29, 2008.
- Yukimoto, S., Yoshimura, H., Hosaka, M., Sakami, T., Tsujino, H., Hirabara, M., Tanaka, T. Y., Deushi, M., Obata, A., Nakano, H., Adachi, Y., Shindo, E., Yabu, S., Ose, T., and Kitoh, A.: Meteorological Research Institute Earth System Model Version 1 (MRI-ESM1) – Model Description –, *Tech. Rep. of MRI*, 64, 83 pp., 2011.
- Zhang, Q., Streets, D. G., He, K., Wang, Y., Richter, A., Burrows, J. P., Uno, I., Jang, C. J., Chen, D., Yao, Z., and Lei, Y.: NO_x emission trends for China, 1995–2004: the view from the ground and the view from space, *J. Geophys. Res.*, 112, D22306, doi:10.1029/2007JD008684, 2007.

**DIAL measurement of
lower tropospheric
ozone**

O. Uchino et al.

Title Page

Abstract

Introduction

Conclusions

References

Tables

Figures

◀

▶

◀

▶

Back

Close

Full Screen / Esc

Printer-friendly Version

Interactive Discussion



Table 1. Characteristics of tropospheric ozone DIAL system.

Transmitter	Nd:YAG (nominal) $70-85 \text{ mJ}$ average				
Pump laser	266 nm				
Wavelength	107 mJ				
Pulse energy	10 Hz				
Pulse repetition rate	8 ns				
Pulse width	CO ₂				
Raman active gas	276 nm 287 nm 299 nm 312 nm				
Stokes lines	7.5 mJ 9.1 mJ 8.4 mJ No. meas.				
Pulse energy	0.1 mrad				
Beam divergence					
Receiver	(after expansion $\times 3.9$)				
Telescope type	Newtonian		Prime focus (fiber coupled)		
Telescope diameter	49 cm		10 cm		
Focal length	1750 mm		320 mm		
Field of view	1 mrad		3 mrad		
Wavelength	287 nm	299 nm	312 nm	276 nm	287 nm
Bandwidth	1.02 nm	1.15 nm	0.82 nm	1.07 nm	1.05 nm
Transmission	0.18	0.32	0.36	0.17	0.21
Detector	PMT (Hamamatsu R3235-01)				
Signal processing	12bit A/D + Photon counting [... MHz]				
Time resolution (raw)	1 min				
Altitude resolution (raw)	7.5 m				

DIAL measurement of lower tropospheric ozone

O. Uchino et al.

Title Page

Abstract

Introduction

Conclusions

References

Tables

Figures

◀

▶

◀

▶

Back

Close

Full Screen / Esc

Printer-friendly Version

Interactive Discussion



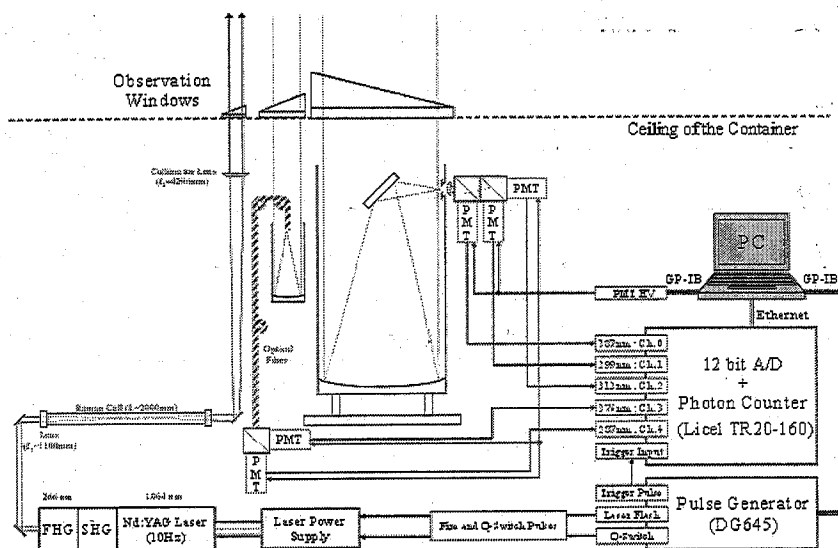


Fig. 1. Block diagram of tropospheric ozone DIAL system.

DIAL measurement of lower tropospheric ozone

O. Uchino et al.

Title Page

Abstract

Introduction

Conclusions

References

Tables

Figures

1

2

3

4

Back

Close

Full Screen / Esc

Printer-friendly Version

Interactive Discussion



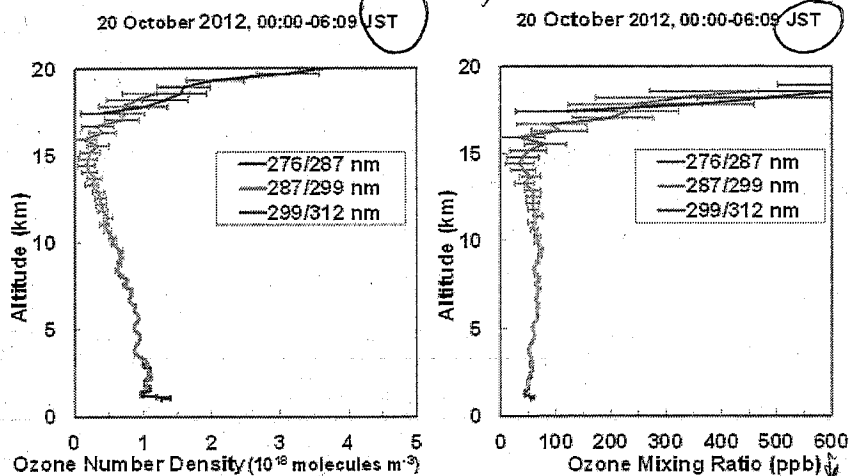


Fig. 2. Vertical profiles of ozone number density (left panel) and ozone mixing ratio (right panel) over Saga observed by DIAL on 20 October 2012. The error bars show the statistical errors calculated from the lidar signal to noise ratios.

10¹³ cm⁻³ = 10¹² cm⁻³

190

1 cm⁻³ = 10¹² cm⁻³

AMTD

7, 171–194, 2014

DIAL measurement of lower tropospheric ozone

O. Uchino et al.

Title Page

Abstract

Introduction

Conclusions

References

Tables

Figures

◀

▶

◀

▶

Back

Close

Full Screen / Esc

Printer-friendly Version

Interactive Discussion



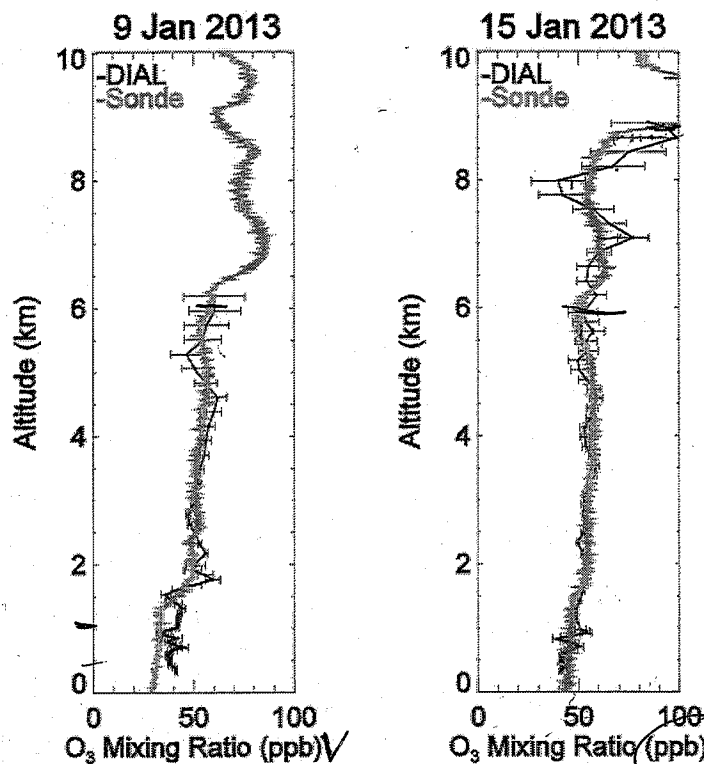


Fig. 3. Comparison of ozone DIAL (black) and ECC ozonesonde (orange) measurements on 9 (left panel) and 15 January (right panel) in 2013. The error bars of ozone DIAL data show the statistical errors calculated from the lidar signal to noise ratios.

Stratospheric?

units in
(ppbv)

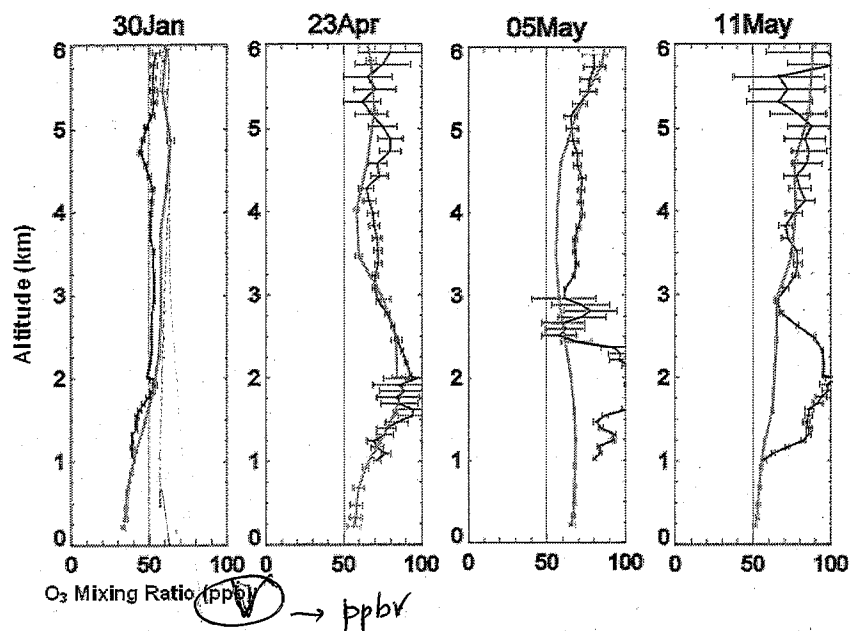


Fig. 4. Vertical profiles of ozone-mixing ratios over Saga measured by DIAL (black lines) and predicted by MRI-CCM2 (orange lines) on 30 January, 23 April, 5 and 11 May in 2012. The error bars shows the statistical errors calculated from the signal to noise ratios for the lidar and the standard deviation for the period predicted by MRI-CCM2.

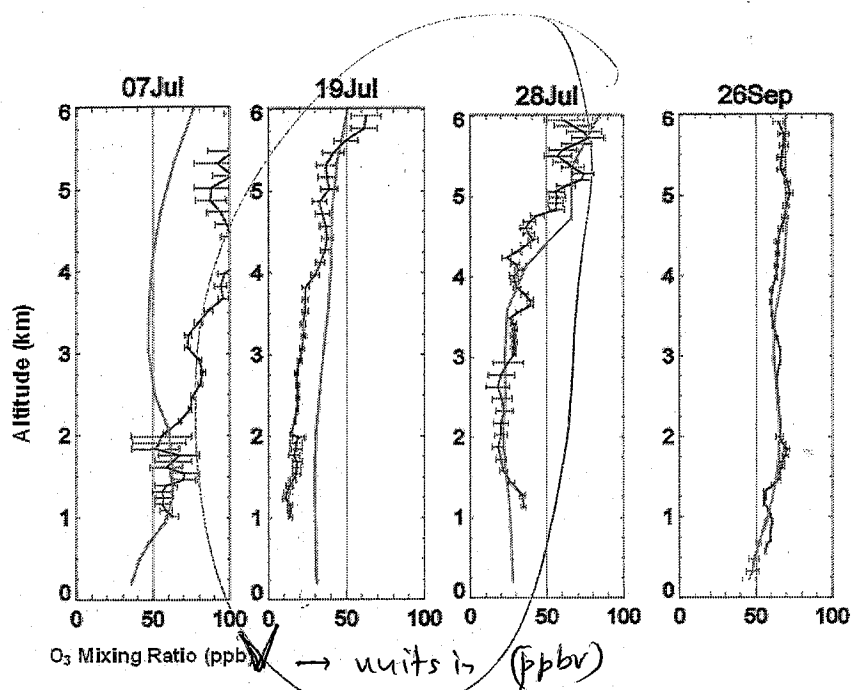


Fig. 5. Same as Fig. 3 but for 7, 19, and 28 July, and 26 September in 2012.

Title Page

Abstract

Introduction

Conclusions

References

Tables

Figures

◀

▶

◀

▶

Back

Close

Full Screen / Esc

Printer-friendly Version

Interactive Discussion



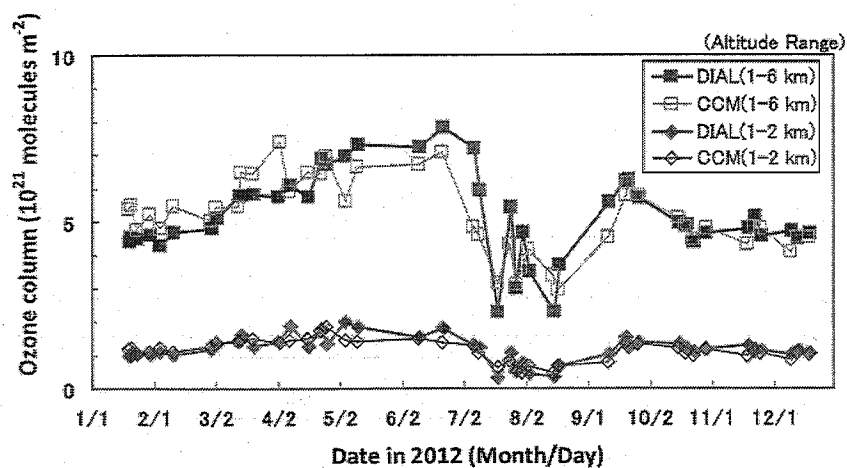


Fig. 6. Ozone columns for 1–6 km and 1–2 km altitude ranges over Saga in 2012 measured by DIAL and predicted by MRI-CCM2.

DIAL measurement of lower tropospheric ozone

O. Uchino et al.

Title Page

Abstract

Introduction

Conclusions

References

Tables

Figures

◀

▶

◀

▶

Back

Close

Full Screen / Esc

Printer-friendly Version

Interactive Discussion

